Chemical Engineering Journal 108 (2005) 91–99

Chemical Engineering Journal

www.elsevier.com/locate/cej

The extended Kalman filter as a noise modulator for continuous yeast cultures under monotonic, oscillating and chaotic conditions☆

Pratap R. Patnaik*

Mathematical Modeling Unit, Institute of Microbial Technology, Sector 39-A, Chandigarh 160036, India

Received 12 May 2004; received in revised form 10 January 2005; accepted 12 January 2005

Abstract

The extended Kalman filter (EKF) is commonly used to filter out the inflow of noise into biological reactors. Its usefulness for bioreactors with monotonic outputs is well established. More recently, the EKF has been shown to be able to rescue stable periodic oscillations that have been distorted by noise. This study extends the use of the EKF to microbial oscillations that become chaotic under the influence of noise. As measured by the Lyapunov exponents of the noise-free and noise-filtered concentration profiles of a continuous culture of *Saccharomyces cerevisiae*, the filter is effective in recovering noise-free sustained oscillations from noise-induced chaos, but is less satisfactory for a culture with both deterministic and stochastic chaos. Other kinds of filters, employing artificial intelligence, are recommended in this case.

Keywords: Extended Kalman filter; Continuous culture; Inflow noise; Oscillations; Chaos

1. Introduction

Under realistic conditions representative of pilot- and industrial-scale operations, continuous cultures of microorganisms are usually under the influence of noise from two main sources. One source is the measurement noise associated with the process sensor signals (pH, temperature, speed of agitation, flow rates, etc.). These are grouped into one noise vector with a particular covariance matrix. The second main source of noise is in the environment, and this usually enters a cultivation vessel or bioreactor through a feed stream. Environmental noise is less predictable and more difficult to characterize than measurement noise. Under open loop control, the two sources of noise do not interact. However, closed loop is often preferred for bioreactors [1]; then the collective impact of measurement noise and inflow noise can seriously injure a fermentation. Although the subject of this study is a continuous culture, batch fermentations are not totally insulated from noise. They provide examples where both kinds of noise simultaneously affect a measurement. For instance, the dosing of alkali or acid for pH control and the flow of a heating or cooling stream for temperature control are influenced by noise from the environment as well as that from the feedback variables which control the switching off or on of these streams. In spite these complexities and their potentially harmful effects on microbial behavior, continuous or fed-batch cultivation is chosen in many cases [1,2] because of economic, kinetic and physiological benefits.

For proper control of a fermentation process, raw noisy data have to be filtered and smoothened to enable optimization and control actions to be applied. Although there are different kinds of noise filters [3], the Kalman filter has been widely used because of its robustness, versatility and effectiveness. A detailed account of its theory is outside the scope of this work and is available elsewhere [4]. Although the most rigorous test of the Kalman filter and its modified version, the extended Kalman filter (EKF), would be in a real production-scale operation, commercial and proprietary restrictions prevent the disclosure of the results of such applications. In view of this difficulty, most studies have applied the Kalman filter either to laboratory-scale bioreactors or to data from such reactors 'corrupted' later by computer-generated noise mim-

☆ IMTECH communication no. 034/2004.

* Tel.: +91 172 2690223; fax: +91 172 22690585/632.
E-mail address: pratap@imtech.res.in.

1385-8947/$ – see front matter © 2005 Elsevier B.V. All rights reserved.
doi:10.1016/j.cej.2005.01.004

Nomenclature

C	intra-cellular storage carbohydrate concentration ($g\,L^{-1}$)
D	dilution rate (h^{-1})
e_i	key enzyme concentration for i-th pathway ($g\,g^{-1}$ biomass)
E	ethanol concentration in the bioreactor ($g\,L^{-1}$)
G	glucose concentration in the bioreactor ($g\,L^{-1}$)
G_0	glucose concentration in the feed stream ($g\,L^{-1}$)
k_La	oxygen mass transfer coefficient (h^{-1})
K_i	Michaelis constant for i-th pathway ($g\,L^{-1}$)
K_{O_2}, K_{O_3}	oxidative pathway oxygen saturation constants ($mg\,L^{-1}$)
O	dissolved oxygen concentration in the bioreactor ($mg\,L^{-1}$)
O^*	dissolved oxygen solubility limit ($mg\,L^{-1}$)
r_i	biomass growth rate on i-th pathway (h^{-1})
S_i	carbon substrate concentration for i-th pathway ($g\,L^{-1}$)
t	elapsed time (h)
u_i	cybernetic variable controlling key enzyme synthesis for i-th pathway
v_i	cybernetic variable controlling key enzyme activity for i-th pathway
X	biomass concentration in the bioreactor ($g\,L^{-1}$)
Y_i	yield coefficient for i-th pathway (g biomass g^{-1} substrate)

Greek letters

α	specific enzyme synthesis rate (h^{-1})
α^*	constitutive enzyme synthesis rate ($g\,h^{-1}$)
β	specific enzyme degradation rate (h^{-1})
φ_i	stoichiometric coefficient for i-th carbon substrate
γ_i	stoichiometric coefficients for storage carbohydrate synthesis and degradation
μ_i	specific growth rate of biomass on i-th substrate (h^{-1})
$\mu_{i,max}$	maximum specific growth rate on i-th substrate (h^{-1})

icking industrial conditions. Despite these limitations, a variety of successful applications establishes the Kalman filter as a useful and reliable technique for noise-affected microbial cultures. These applications cover on-line bioreactor monitoring in conjunction with other methods [5], estimation of respiratory coefficients and specific growth rates of insect cultures [6,7], intracellular protein estimations in plant cell cultures [8], and the development of a time-optimal control system for waste-water treatment [9].

While some of these studies considered either explicitly the intrusion of external noise or implicitly noise that is intrinsic to a sensory device, they have not accounted for the simultaneous effects of both. However, as mentioned before, both sources of noise can be present at the same time, and their cumulative effect on a cultivation process may be more injurious than just an additive effect. For instance, if the two sources of noise resonate with each other and/or with the fermentation process, they may drive a smoothly functioning monotonic culture to chaotic oscillations or initiate run-away behavior [10–12]. Although there are a number of observations of the detrimental effects of noise on cellular processes, only recently have there been efforts toward quantitative analyses of these effects.

Coupling of noise from the environment and from measuring devices can seriously undermine cell viability, reactor stability, productivity and selectivity [11,13,14], besides the possibilities of chaotic oscillations and run-away behavior referred to earlier [10–12]. Although the studies demonstrating these effects cover different microorganisms and different modes of bioreactor operation, they consider only fermentations which generate monotonic profiles with time. Thus, they exclude many important fermentations that show time-dependent oscillations in continuous cultures. Two of the best known in this class are *Zymomonas mobilis* and *Saccharomyces cerevisiae*, with the latter being possibly the most intensively studied and industrially important. So, in this work we investigate the ability of an extended Kalman filter to recreate the original noise-free behavior in continuous cultures of *S. cerevisiae* when the deterministic profiles are (a) monotonic or (b) oscillating or (c) chaotic.

2. Continuous cultures of *S. cerevisiae*

In view of its industrial importance and metabolic complexity, the yeast *S. cerevisiae* has been studied by biochemists, microbiologists and biochemical engineers. Biochemists and microbiologists have unraveled the mechanisms and causes of oscillations intrinsic to the cells. These include features such as cell synchrony [15], the presence of hydrogen sulfide [16] and oxidative phosphorylation [17]. While revealing the metabolic complexities that are at the core of autonomous oscillations, these studies have also underlined the difficulties in formulating comprehensive models that are sufficiently simple to manipulate in automatic control systems.

So, biochemical engineers have tried to blend judiciously lumped metabolic models with bioreactor models that include operational features such as the flow rate (or dilution rate), the rate of supply of oxygen and spatial heterogeneity. The models proposed by Beuse et al. [18], Cazzador et al. [19] and Jones and Kompala [20] are of this kind. While the former two [18,19] are based on proposed mechanisms and a chemical kinetic approach, Jones and Kompala adopted a cybernetic approach.

In the context of bioreactors, cybernetic modeling establishes a formal framework according to the established evolutionary concept that microorganisms try to follow those metabolic pathways that are most favorable to their survival under the prevailing conditions. It also hypothesizes that living cells have at least some rudimentary 'intelligence' that enables them to 'remember' their past experiences and accordingly react to current circumstances. Therefore, two cultures of the same organism but with different histories are likely to respond differently to the same conditions. Cybernetic modeling has been particularly useful in portraying the dynamic behavior of fermentations with more than one kind of cells and/or more than one substrate [21,22].

Owing to its simplicity, physiological closeness to known metabolic concepts, and its ability to depict the observed excursions between different kinds of oscillatory and non-oscillatory behavior under changing conditions, the Jones-Kompala model [20] was used here and in a preceding study [23] to generate data mimicking a noise-affected fermentation and to study the performance of an extended Kalman filter.

Jones and Kompala [20] identified three metabolic pathways by which *S. cerevisiae* may utilize the available carbon sources: glucose fermentation, ethanol oxidation and glucose oxidation. Depending on its past history and the current conditions, the culture may follow either one pathway or two or more pathways to different extents. The current conditions are mainly the dilution rate, the gas–liquid mass transfer rate of oxygen and the degree of mixing of the broth. When there is insufficient glucose, *S. cerevisiae* shifts to ethanol as the main carbon source; while ethanol is synthesized under anaerobic conditions in batch cultures, it can be formed in certain ranges of the oxygen mass transfer rate in continuous cultures [24].

Jones and Kompala [20] determined that with increasing dilution rate the deterministic (noise-free) oscillations decayed in both amplitude and frequency, whereas the oxygen mass transfer coefficient had the opposite effect. Exploration of a wider range of these two manipulated variables shows that, depending on the operating conditions, noise-free continuous cultures of *S. cerevisiae* may display one of three kinds of behavior: monotonic or stable oscillations or chaotic oscillations. When there is noise of sufficiently large intensity in the substrate feed stream, all three forms of fermentation become chaotic. An effective and useful extended Kalman filter should be able to restore substantially the original noise-free performance in all three cases.

Representative monotonic and stable oscillating profiles were chosen from those determined by Jones and Kompala [20]. In each case, two sets of profiles were chosen, one for the dilution rate and the other for the gas–liquid oxygen mass transfer coefficient. Since Jones and Kompala did not present any chaotic deterministic profiles, these were generated by either reducing the dilution rate or increasing the mass transfer coefficient. The onset of chaos was detected by calculating the Lyapunov exponent at each stage. This exponent, whose basis and calculation have been described elsewhere [25], is negative for stable or dissipating systems and positive for chaotic systems. The effectiveness of the Lyapunov exponent for detecting biological chaos has been demonstrated recently [26] for *S. cerevisiae*. It may be noted that the chaotic plots generated at this stage are deterministic since no noise has yet been introduced.

Now, for each of the three types of profiles, Gaussian noise with an adjustable variance and a mean equal to the current deterministic value of the variable of interest was added to the Jones and Kompala [20] model, which was then solved again to obtain the noise-distorted profiles. Adjustability of the variance implies here that this was increased stepwise until the monotonic or oscillating profiles became chaotic.

3. Theory and application of the Kalman filter

The Kalman filter is a set of mathematical equations that provides an efficient recursive solution of the least-squares type. The filter can provide estimations of past, present and future states of a system even when a precise model is not known. This feature is useful for microbial processes under nonideal (realistic) conditions because models developed on laboratory data may become inapplicable or imprecise under the influence of disturbances and spatial gradients [1,27].

The basic Kalman filter addresses the problem of trying to estimate the state $\bar{x}$ of a discrete-time controlled process that is governed by the linear difference equation:

$$\bar{x}_k = \bar{A}\bar{x}_{k-1} + \bar{B}u_k + \bar{w}_{k-1} \tag{1}$$

with a measurement vector that follows:

$$\bar{z}_k = \bar{H}\bar{x}_k + \bar{v}_k \tag{2}$$

In these and later equations, lower case letters with overbars denote vectors while similar capital letters denote matrices. Scalars do not have overbars. $(k-1)$ is the current instant of time and k is the point one time-step ahead. $\bar{w}_k$ and $\bar{v}_k$ represent the process noise and measurement noise respectively.

Previous studies [27–29] show that $\bar{w}_k$ and $\bar{v}_k$ may be represented as white noise with normal probability distributions:

$$p(w) \sim N(0, \bar{Q}) \tag{3}$$

$$p(v) \sim N(0, \bar{R}) \tag{4}$$

where $\bar{Q}$ and $\bar{R}$ are the respective covariance matrices.

Since Eq. (1) applies to linear systems whereas many fermenation (and other biological) processes show a nonlinear behavior, the extended Kalman filter (EKF) was developed. It applies to any nonlinear difference equation of the form:

$$\bar{x}_k = f(\bar{x}_{k-1}, \bar{u}_k, \bar{w}_{k-1}) \tag{5}$$

$$\bar{z}_k = \bar{h}(\bar{x}_k, \bar{v}_k) \tag{6}$$

In principle, the EKF determines the current estimates of a set of variables by linearizing the estimation around the current estimates using the partial derivatives of the process

and measurement functions evaluated at the (known) previous instant of time. The detailed theory and equations are given in the literature [4,30,31]. Note that both Eqs. (1) and (2) and (5) and (6), in pairs, are in discrete form whereas most biological processes are described by continuous models. This is not an impediment because, in practice, data are sampled at discrete points in time. Since the EKF allows any arbitrary variation in the sampling interval, this may be varied according to the nature of the process. For instance, the interval may be made inversely proportional to the current concentration gradient, thus generating closely spaced data when the variations are steep and more widely separated points during mild variations [14].

Earlier studies [14,29,32] have suggested that the feed stream is a major carrier of noise in continuous and fed-batch fermentations, and white noise is the principal component of the observed fluctuations. So, to generate data simulating a noise-influenced oscillating culture, the equations in the Appendix were solved with the parameter values used by Jones and Kompala [20] (see Table 1) and white noise specified by $\bar{Q}$ and $\bar{R}$. Since the measurement covariance $\bar{R}$ pertains to measurement noise in the unfiltered process, this is measured prior to the operation of the filter. Then the application of the filter determines how much this noise has been reduced. The process noise covariance $\bar{Q}$ is more difficult to determine since typically we do not have the ability to observe the process we are estimating. So, based on previous studies [5,8,30], $\bar{Q}$ was set initially to $\bar{Q}_{\mathrm{d}} = ([0.0001 \ldots\ldots 0.0001]^{\mathrm{T}})$ and $\bar{R}$ to $0.003\bar{I}$, where $\bar{I}$ is the identity matrix and $\bar{Q}_{\mathrm{d}}$ is a diagonal matrix. Note that these are starting values and are updated iteratively until the filtered profiles are within acceptable limits of the noise-free profiles. Now, the model of Jones and Kompala [20] has eight concentrations, whose rates of change are expressed by Eqs. (A.6)–(A.11). So $\bar{Q}$ is an (8×8) matrix. Since the glucose and oxygen feed streams are the only inflows to the bioreactor, environmental noise was considered to be present in these two flow rates, thus making $\bar{R}$ a (2×2) matrix. Both $\bar{Q}$ and $\bar{R}$ get updated recursively as shown in Fig. 1 [31].

Apart from its applicability to a nonlinear process, an important distinction between the EKF and the basic discrete Kalman filter is that in the former case the Jacobian $\bar{H}_k$ in the equation for the Kalman gain $\bar{K}_k$ also gets updated with each iteration, thereby speeding up convergence and improving the accuracy of estimations. As explained before, data from the simulated profiles were sampled at intervals inversely proportional to the local concentration gradients, and the tuning of the EKF was updated over successive intervals according to the format in Fig. 1.

Table 1
Values of the parameters [20]

Parameter	Value
α (h^{-1})	1.0
α^* ($g\,h^{-1}$)	0.1
β (h^{-1})	0.2
γ_1 ($g\,g^{-1}$)	6.0
γ_2 ($g\,g^{-1}$)	6.0
γ_3 ($g\,g^{-1}$)	0.3
$\mu_{1,\max}$ (h^{-1})	0.44
$\mu_{2,\max}$ (h^{-1})	0.32
$\mu_{3,\max}$ (h^{-1})	0.31
φ_1 ($g\,g^{-1}$)	0.27
φ_2 ($g\,g^{-1}$)	1.067
φ_3 ($g\,g^{-1}$)	2.087
φ_4 ($g\,g^{-1}$)	0.95
D (h^{-1})	0.16
G_0 ($g\,L^{-1}$)	28.0
k_La (h^{-1})	1200.0
K_1 ($g\,L^{-1}$)	0.1
K_2 ($g\,L^{-1}$)	0.02
K_3 ($g\,L^{-1}$)	0.001
K_{O_2} ($mg\,L^{-1}$)	0.0001
K_{O_3} ($mg\,L^{-1}$)	0.0001
O^* ($mg\,L^{-1}$)	7.5
Y_1 ($g\,g^{-1}$)	0.16
Y_2 ($g\,g^{-1}$)	0.74
Y_3 ($g\,g^{-1}$)	0.50

4. Results and discussion

As mentioned earlier, representative values of the dilution rate (D) and the gas–liquid mass transfer rate of oxygen (k_La) were chosen so as to have for each manipulated variable a monotonic, a stable oscillating and a chaotically oscillating response of the fermentation. These values were 0.05,

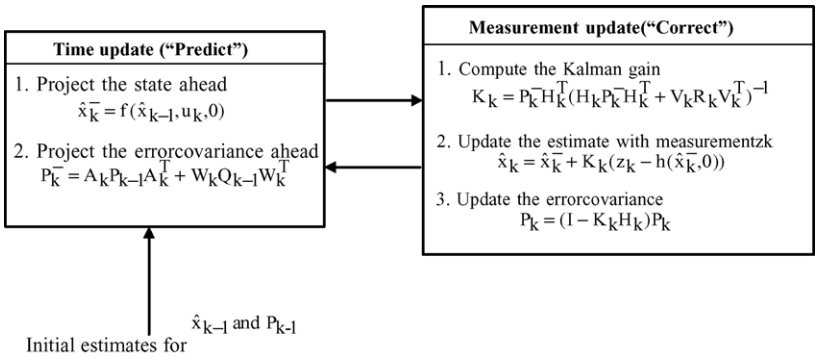

Fig. 1. Computation procedure of the extended Kalman filter [31].

0.13 and 0.20 h^{-1} for the dilution rate, and 175, 255 and 375 h^{-1} for the mass transfer coefficient. The three dilution rates generate chaotic oscillations, stable periodic oscillations and monotonic behavior respectively. These types of profiles are reversed for the mass transfer coefficients, i.e. 375 h^{-1} results in a chaotic response.

Although the model of Jones and Kompala [20] has eight state variables, results for four key concentrations are shown and discussed here, similar to a recent study [33]. This choice also takes care of the internal storage carbohydrate, whose exponents were similar to those for ethanol. Lyapunov exponents computed at three dilution rates (Fig. 2) show that at a low dilution rate (0.05 h^{-1}), the fermentation remains chaotic even after applying the EKF. This is expected because the noise-free fermentation itself had deterministic chaos. However, for the two larger dilution rates the EKF has either fully stabilized the process or has substantially reduced noise-induced chaotic behavior.

A similar performance is seen with respect to the mass transfer coefficient for oxygen (k_La). At $k_La = 375\ h^{-1}$, the culture remains chaotic, as it was before the influx of noise. However, as for the dilution rate, stable performance has been restored in all the cases except two. Including the results (not shown) for internal carbohydrate, these observations show that in 8 out of 10 cases where the noise-free culture was stable (either monotonic or oscillating) the EKF has restored stability after noise had disturbed the process to chaotic oscillation.

Figs. 2 and 3 together depict 24 sets of bar plots covering three dilution rates and three mass transfer coefficients. Twelve of these have been labeled in order to draw closer attention. For low dilution rates (cases 1, 2, 4 and 5 in Fig. 2) and high mass transfer coefficients (cases 7, 9, 11 and 12 in Fig. 3) there is deterministic chaos since the exponents for a fermentation without noise are also positive. In these cases, an EKF cannot be expected to establish stable oscillations. However, its limitation is revealed more significantly in four other cases (3, 6, 8 and 10), where the Lyapunov exponents of the deterministic oscillations are close to zero. Such a system is marginally stable and a disturbance may displace the trajectories such that they either stay at a constant distance from the original noise-free paths or diverge into a chaotic regime [25]. While the former possibility has been observed for monotonic profiles, the Lyapunov exponents determined here suggest that oscillating trajectories are more likely to degenerate into chaos. The difference between the exponents for a noise-free and a noise-filtered system provides a measure of this tendency. The results (Fig. 4) show that for the four cases (3, 6, 8 and 10) where the noise-free culture had steady oscillations with a constant time period, the Lyapunov exponents with an EKF are within 20% of their original values. However, the EKF has been less effec-

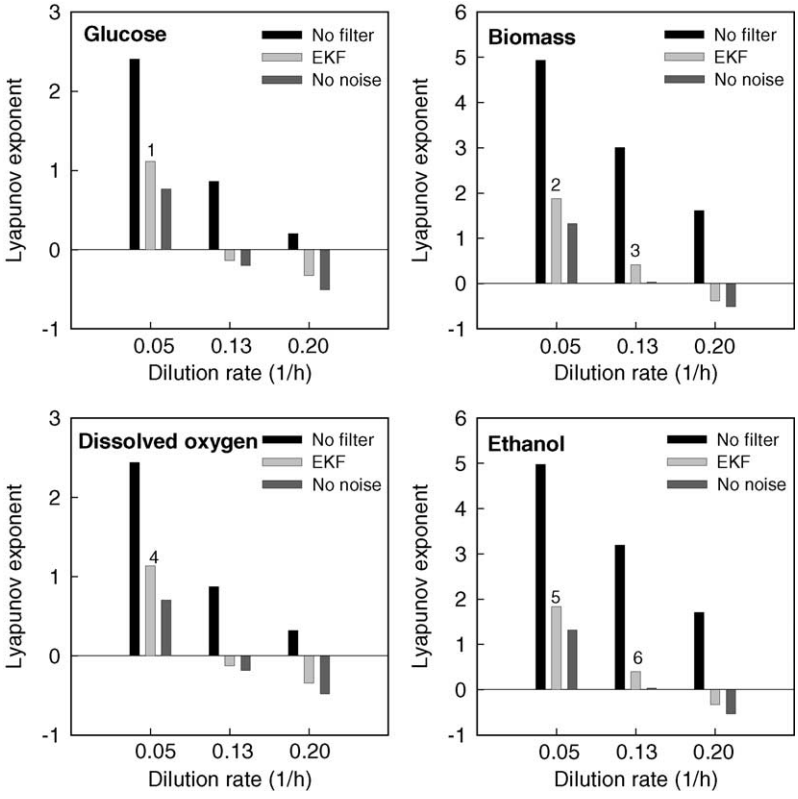

Fig. 2. Lyapunov exponents for a noise-affected fermentation without and with an EKF at dilution rates generating chaotic ($D = 0.05\ h^{-1}$), oscillating ($D = 0.13\ h^{-1}$) and monotonic ($D = 0.20\ h^{-1}$) behavior without noise. In each set of bars, the one on the right is for a fermentation without noise, the bar on the left is with unfiltered noise, and the middle bar pertains to a fermentation with noise filtered by an EKF.

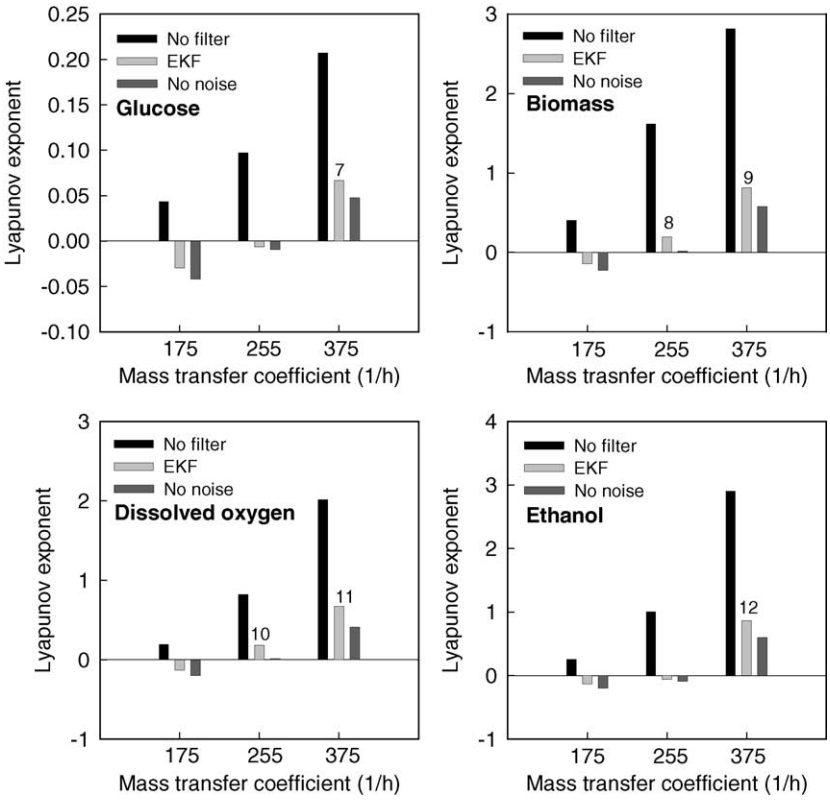

Fig. 3. Lyapunov exponents for a noise-affected fermentation without and with an EKF at mass transfer coefficients generating monotonic ($k_La = 175\,h^{-1}$), oscillating ($k_La = 255\,h^{-1}$) and chaotic ($k_La = 375\,h^{-1}$) behavior without noise. In each set of bars, the one on the right is for a fermentation without noise, the bar on the left is with unfiltered noise, and the middle bar pertains to a fermentation with noise filtered by an EKF.

tive in distinguishing between deterministic chaos and noise-induced chaos, the differences here being about 40–65%. The largest differences are for the dissolved oxygen concentration, which are much smaller in magnitude than the other variables [15,18,20]. This suggests that low concentrations are more difficult to rescue from the effects of noise than high concentrations. This overall inference is however embedded in more complex phenomena involving the cell cycle, the metabolic pathways, the population distribution and interfacial oxygen transfer [15,17,20,34]. Because a model that includes all these features becomes too cumbersome or complex, engineering analyses are based, as stated in Section 2, on judiciously simplified models [18–20]. Even such a model has indicated here that an algorithmic filter such as an EKF may not 'understand' adequately the complexities of a noise-affected microbial process. In such situations, filters that do not depend on a process model may perform better. These are the so-called 'intelligent' filters, which rely on methods such fuzzy logic, neural networks and expert systems. For example, an auto-associative neural filter is better than an EKF and other algorithmic filters in restoring deterministic oscillations from noise-distorted non-chaotic oscillations [35]. Nevertheless, neural filters also have limitations and sometimes a combination of the two may be preferable.

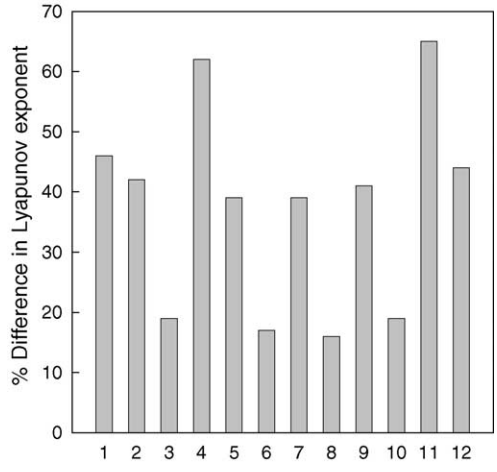

Fig. 4. Differences between the Lyapunov exponents of the noise-free and noise-filtered fermentations for each of the twelve cases labeled in Figs. 2 and 3. Cases 1, 2, 4, 5, 7, 9, 11 and 12 pertain to deterministic chaos.

These differences in the effectiveness of an EKF are also reflected in its ability to converge to the best performance (i.e. as close as possible to that of a noise-free fermentation) through successive iterations. This may be characterized by the mean sum of squares of errors, defined as

$$\mathrm{MSSE}(\%) = \frac{\sum_{j=1}^{N}(X_j^{\mathrm{e}} - X_j^{\mathrm{p}})^2}{N} \times 100 \qquad (7)$$

where X_j^e and X_j^p are respectively the 'experimental' (or simulated) and predicted values of a variable at the j-th sampling point in time, and N is the total number of data. Since, as revealed by their Lyapunov exponents (Figs. 3 and 4), the biomass and ethanol concentrations are distorted by noise to comparable extents and more severely than glucose and dissolved oxygen concentrations, either of the former two may be used to compare the progress of the MSSE for different situations. This comparison (Fig. 5) shows that the EKF is most efficient for deterministic monotonic profiles, less so for steady oscillations and, as expected, the least efficient when both deterministic and noise-induced chaos are present. Nevertheless, it is encouraging to note that an EKF can restore nearly noise-free performance even in the last case.

It may be recalled that the Lyapunov exponent is a measure of the mean deviation between two trajectories. So, to determine whether the deviations without and with an EKF are correlated, Pearson's product moment correlations were calculated as described by Fisher [36]. The correlation between two variables X and Y is defined as

$$\rho_{x,y} = \frac{\mathrm{cov}(X, Y)}{\mathrm{var}(X)\mathrm{var}(Y)} \quad (8)$$

where var stands for variance and cov for covariance.

In our applications, X is the set of noise-free values of any concentration and Y the set of noise-affected values, either without or with an EKF. Since, at each sampling time, every concentration has an unfiltered value and a filtered value, the correlation coefficients between different concentrations generate the matrix presented as Table 2. Since the bioreactor may have any one of three modes of deterministic operation—monotonic, oscillating and chaotic—there are correlation coefficients between each pair of variables.

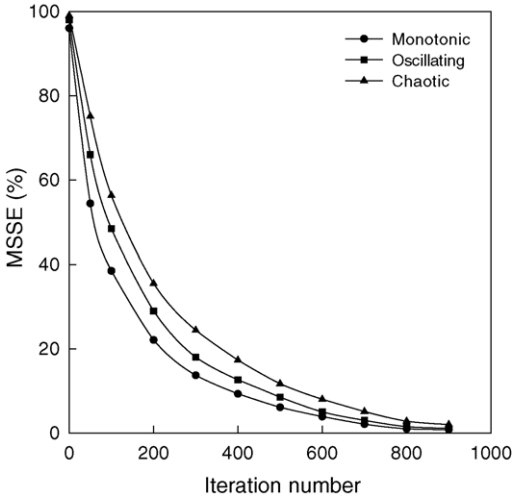

Fig. 5. Convergence profiles for an EKF applied separately to a fermentation under three kinds of deterministic behavior. MSSE: mean sum of squares of errors.

Table 2
Pearson's product moment correlation coefficients between different concentrations in their unfiltered and filtered states

Variable	Mode[a]	Glucose		Biomass		Dissolved oxygen		Ethanol	
		Unfiltered	Filtered	Unfiltered	Filtered	Unfiltered	Filtered	Unfiltered	Filtered
Glucose (unfiltered)	m	1.0	0.993	0.139	0.125	0.128	0.120	0.149	0.138
	o	1.0	0.985	0.123	0.114	0.119	0.111	0.133	0.119
	c	1.0	0.976	0.109	0.101	0.112	0.103	0.124	0.101
Glucose (filtered)	m	0.990	1.0	0.121	0.127	0.122	0.130	0.140	0.147
	o	0.983	1.0	0.113	0.121	0.116	0.125	0.118	0.130
	c	0.976	1.0	0.106	0.114	0.110	0.117	0.106	0.118
Biomass (unfiltered)	m	0.139	0.121	1.0	0.999	0.141	0.132	0.187	0.145
	o	0.123	0.113	1.0	0.999	0.129	0.121	0.175	0.133
	c	0.109	0.106	1.0	0.999	0.117	0.113	0.166	0.122
Biomass (filtered)	m	0.125	0.127	0.999	1.0	0.138	0.151	0.182	0.194
	o	0.114	0.121	0.999	1.0	0.123	0.139	0.173	0.183
	c	0.101	0.114	0.999	1.0	0.109	0.126	0.162	0.170
Dissolved oxygen (unfiltered)	m	0.128	0.122	0.141	0.138	1.0	0.991	0.159	0.137
	o	0.119	0.116	0.129	0.123	1.0	0.986	0.145	0.124
	c	0.112	0.110	0.117	0.109	1.0	0.979	0.133	0.111
Dissolved oxygen (filtered)	m	0.120	0.130	0.132	0.151	0.991	1.0	0.143	0.163
	o	0.111	0.125	0.121	0.139	0.986	1.0	0.132	0.150
	c	0.103	0.117	0.113	0.126	0.979	1.0	0.121	0.139
Ethanol (unfiltered)	m	0.149	0.140	0.187	0.182	0.159	0.143	1.0	0.993
	o	0.133	0.118	0.175	0.173	0.145	0.132	1.0	0.989
	c	0.124	0.106	0.166	0.162	0.133	0.121	1.0	0.984
Ethanol (filtered)	m	0.138	0.147	0.145	0.194	0.137	0.163	0.993	1.0
	o	0.119	0.130	0.133	0.183	0.124	0.150	0.989	1.0
	c	0.101	0.118	0.122	0.170	0.111	0.139	0.984	1.0

[a] m: monotonic; o: oscillating; c: chaotic.

The presence of unity in all elements of three-vectors along the diagonal is expected since any variable will be fully correlated with itself. Large correlation coefficients approaching unity also connect unfiltered and filtered values of the same variable. This too is physically plausible, given that the pair of variables represent the same concentration. All other coefficients are small, indicating the absence of any significant correlation between one concentration and another. These small correlations corroborate the independence of the concentrations in the Jones and Kompala [20] model, and thus Eqs. (A.6)–(A.11) are also independent. Finally, it may be observed that for any variable, its unfiltered value has a higher correlation with the unfiltered value of another variable than with the filtered value of the latter, regardless whether the fermentation displays monotonic or oscillating or chaotic behavior. The same pattern also occurs for all filtered variables. This interesting segregation into two groups with internal consistency strengthens the reliability of the EKF in different situations, but it is difficult to attribute a stronger interpretation.

5. Conclusions

For continuous fermentation by *S. cerevisiae* under deterministic conditions that generate stable periodic oscillations, the EKF has been shown recently to be effective in filtering out noise from the feed stream such that approximately noise-free oscillations can be recovered. Previous studies had already proved this effectiveness for fermentations with monotonic time-domain concentration profiles. So, this study has extended earlier work to sustained oscillations that are driven to chaos under the influence of noise.

Computer-generated data from an experimentally validated cybernetic model of a continuous culture were subjected to Gaussian noise in the substrate feed stream. Three sets of data were generated – monotonic, oscillating and (deterministic) chaotic – by choosing suitable values of the dilution rate or the gas–liquid mass transfer coefficient for oxygen. To each set, an EKF was applied and the extent of recovery of the performance prior to the intrusion of noise was measured by calculating the Lyapunov exponents relating pairs of concentration profiles without noise and with filtered noise.

The EKF restored nearly noise-free performance in eight out of ten cases where this was either monotonic or oscillating periodically. For the two exceptional cases, the Lyapunov exponents of the noise-filtered fermentations were within 20% of those of the corresponding noise-free cultures. However, the EKF was less effective in distinguishing noise-induced chaos from deterministic chaos, to filter out only the former. This limitation may lie in the process model itself, on which the EKF depends. Since very complex models are not desirable and simple models may be inadequate under nonideal conditions, 'intelligent' filters based on expert systems and neural networks that do not require a model may be an answer. To overcome some of the limitations of 'intelligent' filters, they may be combined with partial mathematical descriptions and algorithmic filters to create hybrid filters.

Appendix A. The cybernetic model of Jones and Kompala [20]

Depending on the prevailing conditions, *S. cerevisiae* may follow any one of three metabolic pathways. The rate of growth r_i along each pathway follows modified Monod kinetics, as given below:

Glucose fermentation

$$r_1 = \mu_1 e_1 \left(\frac{G}{K_1 + G}\right) \tag{A.1}$$

Ethanol oxidation

$$r_2 = \mu_2 e_2 \left(\frac{E}{K_2 + E}\right)\left(\frac{O}{K_{O_2} + O}\right) \tag{A.2}$$

Glucose oxidation

$$r_3 = \mu_3 e_3 \left(\frac{G}{K_3 + G}\right)\left(\frac{O}{K_{O_3} + O}\right) \tag{A.3}$$

The pathways are not mutually exclusive and, at a given instant, the organism may follow two or more pathways at different rates. Each pathway is controlled by a key enzyme e_i, with synthesis rate u_i and activity v_i, which follow:

$$u_i = \frac{r_i}{\sum_j r_j} \tag{A.4}$$

$$v_i = \frac{r_i}{\max_j r_j} \tag{A.5}$$

With Eqs. (A.1)–(A.5), the mass balances for a continuous flow bioreactor may be written as follows:

$$\frac{dX}{dt} = \left(\sum_i (r_i v_i) - D\right) X \tag{A.6}$$

$$\frac{dG}{dt} = (G_0 - G)D - \left(\frac{r_1 v_1}{Y_1} + \frac{r_3 v_3}{Y_3}\right) X - \varphi_4 \left(C\frac{dX}{dt} + X\frac{dC}{dt}\right) \tag{A.7}$$

$$\frac{dE}{dt} = -DE + \left(\varphi_1 \frac{r_1 v_1}{Y_1} - \frac{r_2 v_2}{Y_2}\right) X \tag{A.8}$$

$$\frac{dO}{dt} = k_L a(O^* - O) - \left(\varphi_2 \frac{r_2 v_2}{Y_2} + \varphi_3 \frac{r_3 v_3}{Y_3}\right) X \tag{A.9}$$

$$\frac{de_i}{dt} = \alpha u_i \left(\frac{S_i}{K_i + S_i}\right) - \left(\sum_j (r_j v_j) + \beta\right) e_i + \alpha^* \tag{A.10}$$

$$\frac{dC}{dt} = \gamma_3 r_3 v_3 - (\gamma_1 r_1 v_1 + \gamma_2 r_2 v_2)C - \sum_j (r_j v_j)C \quad \text{(A.11)}$$

Inclusion of the term α^* in the enzyme synthesis Eq. (A.10) is based on Turner and Ramkrishna [37], who have shown its importance in predicting the induction of enzymes that have been repressed for long durations. The specific growth rates thus also include α^* in the model:

$$\mu_i = \mu_{i,\max}\left(\frac{\mu_{i,\max} + \beta}{\alpha + \alpha^*}\right) \quad \text{(A.12)}$$

Eq. (A.11) expresses the rate of change of internal storage carbohydrates that are an integral part of the metabolism [24,34].

The φ_i are the stoichiometric coefficients for different substrates S_i, and γ_i are similar coefficients for carbohydrate synthesis and consumption by the cells. Jones and Kompala [20] may be consulted for a full discussion of the model. A point not clarified there is the identification of S_1, S_2 and S_3. Reference to Eqs. (A.1)–(A.3) shows that $S_1 = G$, $S_2 = E$ and $S_3 = G$. This identification is needed to solve the model. The values of the parameters are listed in Table 1.

References

[1] M.L. Shuler, F. Kargi, Bioprocess Engineering. Basic Concepts, Prentice-Hall, New Jersey, 2002.

[2] G. Liden, Understanding the bioreactor, Bioproc. Biosyst. Eng. 24 (2002) 273–279.

[3] O. Nelles, Nonlinear System Identification: From Classical Approaches to Neural Networks and Fuzzy Models, Springer-Verlag, New York, 2000.

[4] M.S. Grewal, A.P. Andrews, Kalman Filtering Theory and Practice, Prentice-Hall, New Jersey, 1993.

[5] L.F.M. Zorzetto, A. Wilson, Monitoring bioprocesses using hybrid models and an extended Kalman filter, Comput. Chem. Eng. 20 (1996) S689–S694.

[6] R. Neeleman, E.J. van den End, A.J.B. Boxtel, Estimation of respiratory coefficient in batch cell cultivation, J. Biotechnol. 80 (2000) 85–95.

[7] R. Neeleman, A.J.B. van Boxtel, Estimation of specific growth rate from cell density measurements, Bioproc. Biosyst. Eng. 24 (2001) 179–185.

[8] J.N. Zhang, W.W. Su, Estimation of intra-cellular phosphate content in plant cell cultures using extended Kalman filter, J. Biosci. Bioeng. 96 (2002) 8–14.

[9] A. Vargas, G. Soto, J. Moreno, G. Buitron, Observer-based time-optimal control of an aerobic SBR for chemical and petrochemical waste treatment, Water Sci. Technol. 42 (2000) 163–170.

[10] P.R. Patnaik, Fractal characterization of the effect of noise on biological oscillations: the biosynthesis of ethanol, Biotechnol. Tech. 8 (1994) 419–424.

[11] P.R. Patnaik, Improvement of the microbial production of streptokinase by controlled filtering of inflow noise, Process Biochem. 35 (1999) 309–315.

[12] S. Sinha, Chaos in biology, Curr. Sci. 73 (1997) 977–983.

[13] P.R. Patnaik, Can imperfections help to improve bioreactor performance? Trends Biotechnol. 20 (2002) 135–137.

[14] P.R. Patnaik, Spectral analysis of the effect of inflow noise on a fed-batch fermentation for recombinant β-galactosidase, Bioprocess Eng. 17 (1997) 93–97.

[15] C.-I. Chen, K.A. McDonald, Oscillatory behavior of *Saccharomyces cerevisiae* in continuous culture, I and II, Biotechnol. Prog. 36 (1990) 19–38.

[16] H.Y. Sohn, D.B. Murray, H. Kuriyama, Ultradian oscillation of *Saccharomyces cerevisiae* during aerobic continuous culture: hydrogen sulfide mediates population synchrony, Yeast 16 (2000) 1185–1190.

[17] J. Wolf, H.Y. Sohn, R. Heinrich, H. Kuriyama, Mathematical analysis of a mechanism for autonomous metabolic oscillations in continuous cultures of *Saccharomyces cerevisiae*, FEBS Lett. 499 (2001) 230–234.

[18] M. Beuse, R. Bartling, A. Kopmann, H. Diekmann, M. Thoma, Effect of dilution rate on the mode of oscillation in continuous cultures of *Saccharomyces cerevisiae*, J. Biotechnol. 61 (1998) 15–31.

[19] L. Cazzador, L. Mariani, E. Martegani, L. Alberghina, Structured segregated models and analysis of self-oscillating yeast continuous cultures, Bioprocess Eng. 5 (1990) 175–180.

[20] K.D. Jones, D.S. Kompala, Cybernetic model of the growth dynamics of *Saccharomyces cerevisiae* in batch and continuous cultures, J. Biotechnol. 71 (1999) 105–131.

[21] P. Doshi, R. Rengaswamy, K.V. Venkatesh, Modelling of microbial growth for sequential utilization in a multi-substrate environment, Process Biochem. 32 (1997) 643–650.

[22] J.V. Straight, D. Ramakrishna, Cybernetic modeling and regulation of metabolic pathways: growth on complementary nutrients, Biotechnol. Prog. 10 (1994) 574–587.

[23] P.R. Patnaik, How effective is an extended Kalman filter for continuous yeast cultures affected by both inflow and measurement noise? Curr. Sci. 86 (2004) 999–1007.

[24] A.D. Satroutdinov, H. Kuriyama, H. Kobayashi, Oscillatory metabolism of *Saccharomyces cerevisiae* in continuous culture, FEMS Microbiol. Lett. 98 (1992) 261–268.

[25] G. Elert, The Chaos Hypertextbook, in: http://hypertextbook.com/chaos, 2000.

[26] P.R. Patnaik, Application of the Lyapunov exponent to detect noise-induced chaos in oscillating yeast cultures, Chaos, Solitons Fractals (2005), in press.

[27] F. Gillard, C. Tragardh, Modeling the performance of industrial bioreactors with a micro-environmental approach: a critical review, Chem. Eng. Technol. 22 (1999) 187–195.

[28] G.A. Montague, A.J. Morris, Neural network contributions in biotechnology, Trends Biotechnol. 12 (1994) 312–324.

[29] M. Rohner, H.-P. Meyer, Application of modelling for bioprocess design and control in industrial production, Bioproc. Eng. 13 (1995) 69–78.

[30] G. Stephanopoulos, S. Park, Bioreactor state estimation, in: K. Schugerl (Ed.), Biotechnology. Measuring, Modeling and Control, vol. 4, VCH, Weinheim, 1992, pp. 225–249.

[31] G. Welch, G. Bishop, An introduction to the Kalman filter. http://www.cs.unc.edu/~welch/media/pdf/kalman_intro.pdf, 2004.

[32] A. Lubbert, R. Simutis, Using measurement data in bioprocess modelling and control, Trends Biotechnol. 12 (1994) 304–311.

[33] P.R. Patnaik, A Lyapunov comparison of noise-filtering methods for oscillating yeast cultures, AIChE J. 50 (2004) 1640–1646.

[34] P. Duboc, I. Marison, U. von Stochar, Physiology of *Saccharomyces cerevisiae* during cell cycle oscillations, J. Biotechnol. 51 (1996) 57–72.

[35] P.R. Patnaik, On the performances of noise filters in the restoration of oscillatory behavior in continuous yeast cultures, Biotechnol. Lett. 25 (2003) 681–685.

[36] L. Fisher, in: C.E. Pearson (Ed.), Handbook of Applied Mathematics, Van Nostrand, New York, 1990 (Chapter 21).

[37] B.G. Turner, D. Ramkrishna, Revised enzyme synthesis rate expression in cybernetic models of bacterial growth, Biotechnol. Bioeng. 31 (1988) 41–43.